

Effects of neutron richness on the behavior of nuclear systems at intermediate energies

G. Cardella,² G. Giuliani,^{2,3} I. Lombardo,^{4,*} M. Papa,² L. Acosta,¹ C. Agodi,¹ F. Amorini,¹ A. Anzalone,¹ L. Auditore,⁵ I. Berceanu,⁸ S. Cavallaro,^{1,3} M. B. Chatterjee,⁹ E. De Filippo,² E. Geraci,^{2,3} L. Grassi,^{2,3} J. Han,¹ E. La Guidara,^{2,7} D. Loria,⁵ G. Lanzalone,^{1,6} C. Maiolino,¹ T. Minniti,⁵ A. Pagano,² S. Pirrone,² G. Politi,^{2,3} F. Porto,^{1,3} F. Rizzo,^{1,3} P. Russotto,^{1,3} S. Santoro,⁵ A. Trifirò,⁵ M. Trimarchi,⁵ G. Verde,² and M. Vigilante⁴

¹*INFN, Laboratori Nazionali del Sud, Via S. Sofia, Catania, Italy*

²*INFN, Sezione di Catania, Via S. Sofia, 95123 Catania, Italy*

³*Dip. di Fisica e Astronomia, Università di Catania, Via S. Sofia, Catania, Italy*

⁴*Dip. di Scienze Fisiche, Università di Napoli Federico II, and INFN-Sezione di Napoli, Italy*

⁵*Dip. di Fisica, Università di Messina and INFN, Gr. Coll. Messina, Italy*

⁶*Facoltà di Ingegneria ed Architettura, Università Kore, Enna, Italy*

⁷*Centro Siciliano di Fisica Nucleare e Struttura della Materia, Catania, Italy*

⁸*Institute for Physics and Nuclear Engineering, Bucharest, Romania*

⁹*Saha Institute of Nuclear Physics, Kolkata, India*

(Received 3 May 2012; published 12 June 2012)

We discuss results concerning the behavior of hot nuclear sources formed in $^{40,48}\text{Ca} + ^{40,48}\text{Ca}$ reactions at 25 MeV/nucleon. A correlation between the neutron-to-proton ratio of the total systems and heavy residue production is found. This correlation underlines the strong role played by the neutron-to-proton ratio degree of freedom on the behavior of hot nuclei at intermediate energies. Comparisons of our data with Constrained Molecular Dynamics calculations confirm that a moderately stiff behavior of the symmetry potential must be used to reproduce experimental data. These findings open the way for future investigations with exotic beams at radioactive ion beam facilities.

DOI: [10.1103/PhysRevC.85.064609](https://doi.org/10.1103/PhysRevC.85.064609)

PACS number(s): 25.70.Lm, 25.70.Pq

I. INTRODUCTION

The evolution of hot nuclear systems formed near limiting conditions of excitation energy was considered one of the most fascinating topics in Nuclear Physics in recent decades [1,2]. Thermodynamical [3,4] and dynamical [5,6] approaches have been developed to describe the behavior of hot nuclear sources formed in nuclear reactions at bombarding energies near 20–30 MeV/nucleon [7].

In this energy domain, reactions between medium mass nuclei (as Calcium isotopes) lead to massive transfer and/or incomplete fusion phenomena [8–13]. The formed sources are highly excited, up to the limits of existence of bound systems [14]. The production of heavy residue remnants is in competition with other reaction mechanisms, such as the production of two or more fragments [15–20], and it practically disappears at higher energy [21,22].

A long time ago it was proposed that neutron richness of systems formed in the first phase of the collision could play a key-role in the evolution of reaction dynamics [3,23]. The study of isospin effects can be very useful to extract information about the behavior of the symmetry energy term in the nuclear equation of state [24–29].

To better understand the role of the neutron to proton ratio (N/Z) degree of freedom on the dynamical evolution of semicentral reactions, we decided to study cases involving stable medium mass beam and target nuclei. In particular, we concentrated our attention on reactions involving calcium

isotopes. They allow us to investigate the behavior of a symmetric system ($^{40}\text{Ca} + ^{40}\text{Ca}$, $N/Z = 1$) with the same number of neutrons and protons, as well as the very neutron rich system $^{48}\text{Ca} + ^{48}\text{Ca}$, having $N/Z = 1.4$. We studied also the mixed systems $^{40}\text{Ca} + ^{48}\text{Ca}$ and $^{48}\text{Ca} + ^{40}\text{Ca}$ in order to have intermediate reference points and to evaluate kinematical effects. All these reactions were performed at 25 MeV/nucleon bombarding energy; reaction products were detected by means of the 4π multidetector array Chimera. We compared experimental data to Constrained Molecular Dynamics (CoMD-II) [30] model calculations already used in Ref. [31]. From the comparison, we extracted information about the behavior of the symmetry energy of the nuclear equation of state at near-saturation densities.

II. EXPERIMENTAL DETAILS

The experiment was performed at the Super-Conductive Cyclotron facility of INFN-Laboratori Nazionali del Sud (Catania, Italy). Beams of ^{40}Ca and ^{48}Ca accelerated at 25 MeV/nucleon impinged on self-supporting isotopically enriched targets of ^{40}Ca and ^{48}Ca (1.2 and 2.7 mg/cm² thick, respectively). We used the 4π multidetector Chimera [32,33] as a detection device. It is constituted by 1192 Si-CsI(Tl) telescopes, covering $\simeq 94\%$ of the whole solid angle. Details about the array and its detection and identification capabilities are described in Refs. [32–36]. Masses of heavy residues, which are stopped in silicon detectors, have been measured by means of the time-of-flight technique. The obtained time resolution is ≈ 1 ns (as seen from elastic scattering at forward directions),

*ivlombardo@na.infn.it

including the pulsed beam time resolution. The obtained mass resolution ($\frac{\Delta m}{m}$) is around 5% [31] for nuclei having mass $A \approx 50$, typical of heavy residues detected in the explored reactions. In this experiment, the emitted fragments have been detected starting from $\theta_{\text{lab}} \geq 4.6^\circ$. For this reason, the very forward part of heavy residue emission (principally belonging to fusion-evaporation events) could be partially underestimated. However, due to similar kinematics involved, this effect should be very similar for the various studied systems.

We analyzed only complete events, where the total detected charge Z_{tot} was larger than 80% of entrance charge ($32 \leq Z_{\text{tot}} \leq 40$) and the total reconstructed momentum was at least 70% of the entrance momentum. Quasi-elastic reactions were strongly reduced during the experiment by an appropriate electronics trigger condition, requiring the detection of at least three charged particles. Silicon energy calibrations were obtained by using elastic scattering of beams at various energies, combined with calibrated pulser signals. Their quality was moreover checked with punch-through energies of different nuclear species.

III. HEAVY RESIDUE EMISSION

Semicentral events of reaction have been selected according to criteria already used in Refs. [31,37,38] and based on charged particle multiplicity (m_{cp}) [39] and fragment velocity selections. The global behavior of m_{cp} distributions is similar for all the studied reactions even if, for the neutron-rich systems, the m_{cp} distributions are slightly shifted to lower values. This effect, as already discussed in Ref. [31], could be attributed to the larger probability of emitting neutrons (that are undetected) in neutron-rich systems. For this reason, to analyze events that can be associated to similar windows of impact parameters, we selected events having $m_{\text{cp}} \geq 6$ for $^{40}\text{Ca} + ^{40}\text{Ca}$ reaction and $m_{\text{cp}} \geq 5$ for the other reactions. In order to isolate massive transfer phenomena, leading to the simultaneous presence of a very excited source and a quasiprojectile remnant [40], we analyzed the class of events where the second or the third biggest fragment has a velocity larger than 1.3 times the center of mass velocity, $v > 1.3v_{\text{CM}}$. For this class of events, we show in Fig. 1 mass distributions, m_1 , of the biggest emitted fragment (BEF) for the studied systems; a window on the velocity of the BEF (v_1) is used to discard quasiprojectile and quasitarget contaminations ($0.04 < \frac{v_1}{c} < 0.15$).

Apart from obvious effects due to the different mass of entrance channels (Fig. 1, left panel) that can be reduced by normalizing m_1 to the total mass of the systems m_{tot} (Fig. 1, right panel), an interesting different behavior is observed. Heavy residues (characterized by a mass larger than the projectile one, $m_1/m_{\text{tot}} \approx 0.6$) are emitted with large probability in the very neutron-rich system $^{48}\text{Ca} + ^{48}\text{Ca}$, while the emission of fragments with mass smaller than the projectile/target one prevail in the $N = Z$ system $^{40}\text{Ca} + ^{40}\text{Ca}$. Such relatively small fragments can be produced in binary-like, fusion-fission or multifragmentation events. From thermometric and calorimetric analysis of incomplete fusion events studied in $^{40}\text{Ca} + ^{40}\text{Ca}$ and $^{40}\text{Ca} + ^{48}\text{Ca}$ reactions, rather

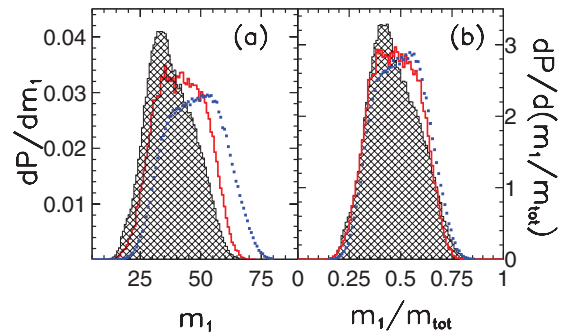


FIG. 1. (Color online) (a) Mass distribution of the biggest emitted fragment (BEF) in the selected class of semicentral events. Black shaded histogram: $^{40}\text{Ca} + ^{40}\text{Ca}$. Red solid histogram: $^{40}\text{Ca} + ^{48}\text{Ca}$. Blue dots: $^{48}\text{Ca} + ^{48}\text{Ca}$. (b) Distributions of normalized mass m_1/m_{tot} of the BEF in the studied collisions for the same class of events. In both panels, y axis have been normalized to the total number of counts and to the width of the bins. Mass evaluation is affected by 5% error, as discussed in the text.

similar temperatures and excitation energy distributions have been obtained [37,38]. We verified moreover that the studied effect is not biased by the different selection criteria applied on charged particle multiplicity.

In order to quantify the competition between the various reaction mechanisms observed experimentally, we have attempted (as a first approximation) to reproduce the shape of experimental m_1 spectra by the superimposition of two Gaussian distributions [see Figs. 2(a)–2(d)] for all the studied systems. As can be better evidenced in the $^{40}\text{Ca} + ^{40}\text{Ca}$ case, the first gaussian is centered at low m_1 values ($m_1 \approx 35$). The second one, more evident in the $^{48}\text{Ca} + ^{48}\text{Ca}$ case, is centered at higher m_1 values ($m_1 \approx 50$ – 55). This contribution can be

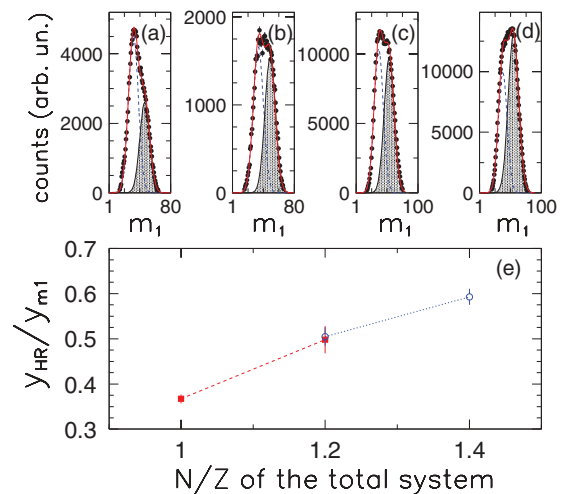


FIG. 2. (Color online) (a,b,c,d) Mass distributions of the BEF in the selected semicentral events. Black dots: experimental data. Blue dashed line: binary-like and multifragmentation contribution. Shaded Gaussian: heavy-residue production. Red solid line: two Gaussian fit. (a) $^{40}\text{Ca} + ^{40}\text{Ca}$, (b) $^{40}\text{Ca} + ^{48}\text{Ca}$, (c) $^{48}\text{Ca} + ^{40}\text{Ca}$, and (d) $^{48}\text{Ca} + ^{48}\text{Ca}$ cases. (e) Heavy-residue yields normalized to the total yield of selected events and obtained from the fit procedure, as a function of the N/Z of analyzed systems.

associated to heavy-residue production in incomplete fusion phenomena. Following this assumption, we can evaluate the relative yield of heavy residues with respect to other reaction mechanisms by comparing the integral of this second Gaussian to the total selected event yield ($y_{\text{HR}}/y_{\text{m1}}$). This value is plotted in Fig. 2(e) as a function of the total N/Z of the colliding systems. A clear correlation is observed. In particular, in the case of neutron-rich $^{48}\text{Ca} + ^{48}\text{Ca}$ reaction ($N/Z = 1.4$), the probability of heavy-residue production is approximately 1.6 times larger than the case of $^{40}\text{Ca} + ^{40}\text{Ca}$ reaction ($N/Z = 1.0$). Mixed systems $^{40}\text{Ca} + ^{48}\text{Ca}$ and $^{48}\text{Ca} + ^{40}\text{Ca}$, having an intermediate N/Z ratio ($N/Z = 1.2$), show an intermediate behavior. This effect underlines the fundamental role played by the N/Z degree of freedom on the production of heavy residues by nuclear systems formed at 25 MeV/nucleon bombarding energy.

It is possible to study the competition between various reaction mechanisms also by inspecting the behavior of ΔM_{nor} spectra [31]. $\Delta M_{\text{nor}} \equiv \frac{m_1 - m_2}{m_{\text{tot}}}$ is the mass difference of the two BEF, normalized to the total mass of entrance channel. From this definition, we infer that high values of ΔM_{nor} are correlated mainly to events with HR emission, while on the contrary low values of ΔM_{nor} are associated to binary-like, multifragmentation and fusion-fission phenomena [31]. In Fig. 3 we show the behavior of ΔM_{nor} spectra for the selected semicentral events of $^{40}\text{Ca} + ^{40}\text{Ca}$, $^{40}\text{Ca} + ^{48}\text{Ca}$, and $^{48}\text{Ca} + ^{48}\text{Ca}$ reactions. We observe that, by increasing the neutron content of the entrance channels, ΔM_{nor} distributions are pushed to higher values, i.e., the emission of a HR is

prevailing on other reaction mechanisms. In a sharp approximation, we can suppose that the region of the spectrum with $\Delta M_{\text{nor}} \geq 0.4$ is associated mainly with events where HR are emitted. Following this assumption, we can estimate (in a way alternative to the two-gaussian fit previously discussed) the relative yield of heavy residues with respect to other reaction mechanisms as a function of the N/Z of the entrance channel. This is shown in the inset of Fig. 3 (solid stars). The behavior obtained is similar to that of Fig. 2(e); i.e., an increasingly higher probability of observing HR emission in the selected semicentral events is seen by increasing the neutron richness of the total system formed in the collision.

In a qualitative way, we can explain the observed effect by considering that, in the very neutron-rich $^{48}\text{Ca} + ^{48}\text{Ca}$ system, the systems formed in the first phase of the collision are pushed close to the stability valley, while for the $^{40}\text{Ca} + ^{40}\text{Ca}$ case, they are closer to the proton drip line. To evidence effects due to the interplay between Coulomb and Symmetry terms in nuclear dynamics, we compared experimental data to dynamical model calculations, as described in the following section.

IV. COMPARISON WITH COMD-II MODEL CALCULATIONS

In our previous works [31] and other theoretical works [41,42], it has been pointed out that the competition between heavy-residue production and other reaction mechanisms is heavily sensitive to the different stiffness options used to describe the density dependent part of the symmetry potential in the nuclear equation of state. In Ref. [31], by comparing our data with Constrained Molecular Dynamics (CoMD-II) model calculations, we found that a moderately stiff option of the symmetry potential must be used to reproduce successfully experimental distributions related to the masses of the largest fragments emitted in semicentral events of $^{40}\text{Ca} + ^{40,48}\text{Ca}$ reactions. We can now extend the analysis to the new $^{48}\text{Ca} + ^{48}\text{Ca}$ data discussed above.

In the CoMD-II model, the symmetry interaction is microscopically derived starting from the different neutron-neutron, proton-proton, and neutron-proton interactions. This allows us to also point out the key role played by nuclear correlations to describe the effects related to the symmetry potential in heavy ion collisions [41]. The various form factors describing the density-dependent part of the symmetry potential have the same functional form adopted in equation of state static calculations [43] and typically used in mean-field models as the Boltzmann-Uheling-Uhlenbeck one (BUU) [44]. As shown in Refs. [31,41], for near-saturation densities it is possible to approximate the form factor of the symmetry potential as $(\frac{\rho}{\rho_0})^\gamma$, where the so-called Stiff1, Stiff2, and Soft options correspond to $\gamma = 1.5, 1.0, 0.5$, respectively. The total value of the symmetry energy strength used is around 40 MeV. The dynamical evolution of the analyzed system has been determined up to 600 fm/c. To take into account the de-excitation phase of primary fragments simulated with CoMD-II model, we used the GEMINI code with standard parameters. Simulated events have been filtered by taking into account the efficiency of the experimental apparatus and the main selection criteria adopted in the analysis of experimental data.

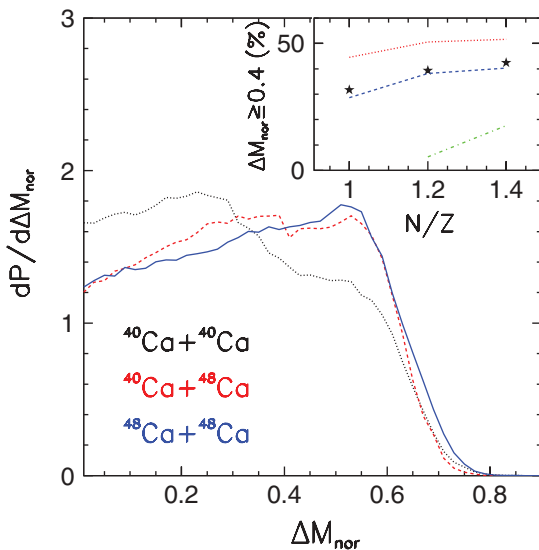


FIG. 3. (Color online) Comparison of experimental ΔM_{nor} distributions for selected semicentral events of $^{40}\text{Ca} + ^{40}\text{Ca}$ (black dots), $^{40}\text{Ca} + ^{48}\text{Ca}$ (red dashes), and $^{48}\text{Ca} + ^{40}\text{Ca}$ (blue solid line) reactions. In the insert, we show the probability of populating the $\Delta M_{\text{nor}} \geq 0.4$ region (typical of HR events) as a function of the N/Z of the total system. Solid stars are experimental data, while lines are the predictions of CoMD-II model calculations performed by using different options for the stiffness of the symmetry potential: Stiff1 (red dotted line), Stiff2 (blue dashed line), and Soft (green dash-dotted line).

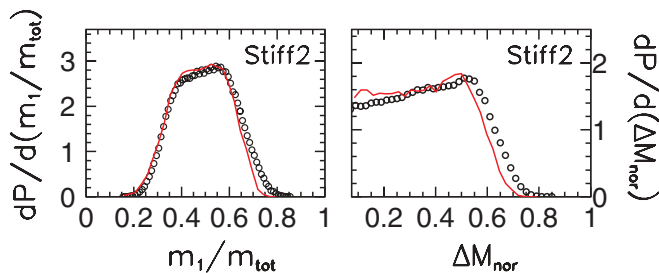


FIG. 4. (Color online) Comparison of experimental mass distributions m_1/m_{tot} and ΔM_{nor} (black dots) with results obtained from CoMD-II + GEMINI [45] calculations (red line) for the case of $^{48}\text{Ca} + ^{48}\text{Ca}$ reaction. Stiff2 parametrization is used to describe density dependence of symmetry potential.

In Fig. 4 (left-hand side) we see that the Stiff2 option (corresponding to $\gamma = 1.0$) well approximate the experimental m_1/m_{tot} distribution (dots). This is in good agreement with previous investigations [31] on the other studied systems $^{40}\text{Ca} + ^{40,48}\text{Ca}$.

An even more stringent test is provided by considering the correlations between the masses of the first and second BEF. To do this, we can use the ΔM_{nor} quantity, defined in the previous paragraph. As shown in Fig. 4 (right panel), CoMD-II calculations, with Stiff2 option (red line), reproduces quite well the magnitude and the global shape of such experimental data (dots), except for the largest ΔM_{nor} values. Also, the integral of the $\Delta M_{\text{nor}} \geq 0.4$ region (that can be associated to events with HR emission) is well reproduced, as shown in the insert of Fig. 3. As in Ref. [31], we performed CoMD-II calculations without the final GEMINI stage and we find that the effect of the de-excitation code on the simulated data consists mainly in a shift of the peaks of mass distributions to slightly lower values. However, the overall shape of mass and ΔM_{nor} distributions remains unaltered.

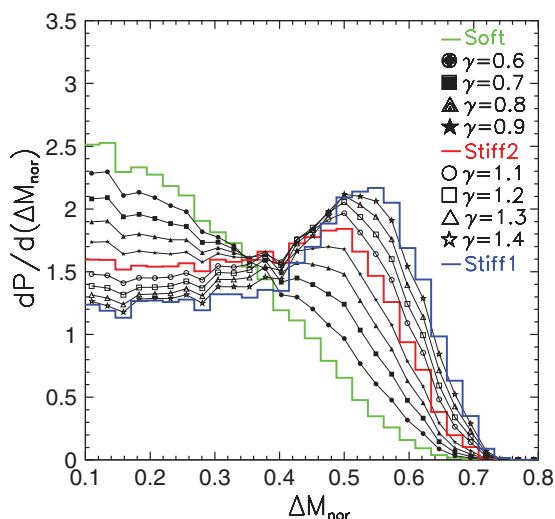


FIG. 5. (Color online) Theoretical ΔM_{nor} distributions, for the $^{48}\text{Ca} + ^{48}\text{Ca}$ reaction. Stiff1, Stiff2, and Soft options are shown (blue, red, and green thick lines, respectively), together with interpolations corresponding to stiffness parameters $0.6 \leq \gamma \leq 1.4$ (filled and empty symbols).

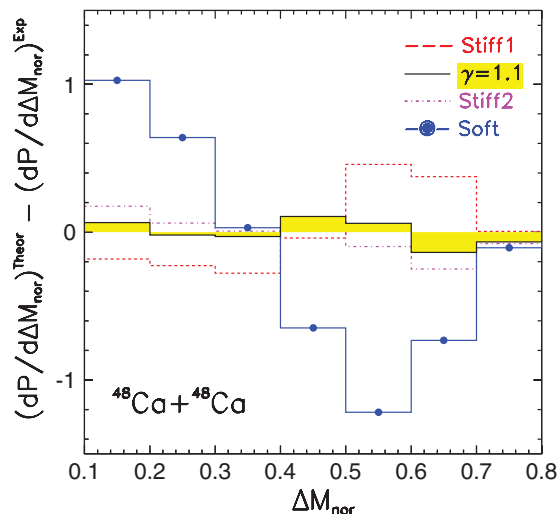


FIG. 6. (Color online) Deviation between theoretical and experimental ΔM_{nor} distributions, for different choices of the symmetry potential stiffness. Dashed-dotted fuchsia histogram: Stiff2 option is used. Red dashed histogram: Stiff1 option. Blue dots: soft option. Filled area histogram: $\gamma = 1.1$.

Starting from the three available options for the symmetry potential, it is possible to determine the behavior of ΔM_{nor} spectra for intermediate values of the stiffness γ parameter by interpolating, bin per bin, the calculations. The result of this procedure is shown in Fig. 5, where we plot spectra obtained for γ parameters ranging from 0.5 to 1.5 at 0.1 step.

The difference between theoretical and experimental ΔM_{nor} distributions, $(\frac{dP}{d\Delta M_{\text{nor}}})^{\text{Theor}} - (\frac{dP}{d\Delta M_{\text{nor}}})^{\text{Exp}}$ (Fig. 6) allows us to better disentangle the effects due to the different stiffness options. By analyzing Fig. 6, it appears rather clearly that Stiff1 option overestimates heavy-residue production (i.e., the region at large ΔM_{nor} values, see also Sect. II), while by using Soft option the production of events with two or more big fragments (low ΔM_{nor} values) is strongly overestimated.

We may refine the estimate of γ parameter by studying deviation spectra obtained by using theoretical distributions that correspond to interpolated γ values. We choose as better estimate the γ parameter leading to the minimum deviation as compared to experimental data. In our case, this requirement is satisfied by the ΔM_{nor} distribution corresponding to an interpolated stiffness value $\gamma = 1.1$ (see Fig. 6, filled histogram). For this reason, we evaluated a value of the stiffness parameter $\gamma = 1.1 \pm 0.1$ as the best suited to reproduce experimental data concerning $^{48}\text{Ca} + ^{48}\text{Ca}$ reaction. This analysis, in agreement with our previous estimates reported in Ref. [31] for the $^{40}\text{Ca} + ^{40,48}\text{Ca}$ systems, confirms that a moderately stiff behavior of the form factor of the symmetry potential has to be used to reproduce correctly experimental data at near-saturation densities ($\rho_0 \pm 0.15\rho_0$, according to CoMD-II model predictions).

V. CONCLUSIONS AND PERSPECTIVES

In conclusion, the fate of hot nuclear sources formed in semicentral reactions was investigated by studying heavy

residue production in nuclear reactions involving different Calcium isotopes at 25 MeV/nucleon, i.e., at the entrance of the Fermi energy domain. The competition between heavy-residue production and other reaction mechanisms is different for the studied systems, and it could be attributed mainly to the difference in the neutron-to-proton ratio of the used entrance channels. By increasing the neutron content of the total system, heavy residue production increases to the detriment of other reaction mechanisms (two or more fragment production). In a previous work [31], we verified, also by using the $^{40}\text{Ca} + ^{46}\text{Ti}$ system, that the observed effect is barely biased by the different total mass of the studied systems.

The comparison of experimental data with CoMD-II model calculations confirms that, as a result of two-body neutron-proton correlations, a moderately stiff behavior of the density dependent part of symmetry potential must be used to reproduce the data.

As a perspective, it would be very useful to enlarge the N/Z range of entrance channels by exploring heavy-residue production in nuclear collisions performed by using neutron-rich and proton-rich radioactive beams in the region of calcium. It would be also very interesting to enlarge the range of the experimental data to lower bombarding energies, in order to study the effects of the N/Z degree of freedom on the competition between fusion-evaporation and fusion-fission processes following medium-mass compound nuclei formation.

ACKNOWLEDGMENTS

We acknowledge D. Rifuggiato and coworkers for the excellent timing properties of beams and C. Marchetta and E. Costa for providing high-quality targets. We thank E. Rosato for valuable comments and discussions about the subject of this paper.

-
- [1] D. A. Bromley, *Treatise on Heavy Ion Science* (Plenum Press, NY, 1984), Vol. 2, Chap. 3.
- [2] R. Dayras *et al.*, *Nucl. Phys. A* **460**, 299 (1986).
- [3] S. Levit and P. Bonche, *Nucl. Phys. A* **437**, 426 (1985).
- [4] J. Besprosvany and S. Levit, *Phys. Lett. B* **217**, 1 (1989).
- [5] M. Papa *et al.*, *Phys. Rev. C* **68**, 034606 (2003).
- [6] M. Colonna, M. Di Toro, G. Fabbri, and S. Maccarone, *Phys. Rev. C* **57**, 1410 (1998).
- [7] B. Borderie and M. F. Rivet, *Prog. Part. Nucl. Phys.* **61**, 551 (2008).
- [8] H. Morgenstern, W. Bohne, W. Galster, K. Grabisch, and A. Kyanowski, *Phys. Rev. Lett.* **52**, 1104 (1984).
- [9] H.-J. Keim, B. Kohlmeier, H. Stege, H. A. Bossler, F. Puhlhofer, and W. F. W. Schneider, *Z. Phys. A* **327**, 101 (1987).
- [10] M. F. Rivet, B. Borderie, H. Gauvin, D. Gardes, C. Cabot, F. Hanappe, and J. Peter, *Phys. Rev. C* **34**, 1282 (1986).
- [11] M. Gonin, J. P. Coffin, G. Guillaume, F. Jundt, P. Wagner, P. Fintz, B. Heusch, A. Malki, A. Fahli, S. Kox, F. Merchez, and J. Mistretta, *Phys. Rev. C* **38**, 135 (1988).
- [12] M. D'Agostino *et al.*, *Nucl. Phys. A* **861**, 47 (2011).
- [13] S. Pirrone *et al.*, *Phys. Rev. C* **64**, 024610 (2001).
- [14] G. Nebbia *et al.*, *Phys. Rev. C* **45**, 317 (1992).
- [15] L. Shvedov, M. Colonna, and M. Di Toro, *Phys. Rev. C* **81**, 054605 (2010).
- [16] C. Ngô, *Nucl. Phys. A* **488**, 233c (1988).
- [17] D. Jouan *et al.*, *Z. Phys. A* **340**, 63 (1991).
- [18] P. Laitesse *et al.*, *Phys. Rev. C* **71**, 034602 (2005).
- [19] G. Ademard *et al.*, *Phys. Rev. C* **83**, 054619 (2011).
- [20] S. Pirrone *et al.*, *EPJ Web Conferences* **17**, 16010 (2012).
- [21] P. Laitesse *et al.*, *Eur. Phys. J. A* **27**, 349 (2006).
- [22] R. K. Puri and S. Kumar, *Phys. Rev. C* **57**, 2744 (1998).
- [23] M. Farine, T. Sami, B. Remaud, and F. Sebille, *Z. Phys. A* **339**, 363 (1989).
- [24] M. B. Tsang, Yingxun Zhang, P. Danielewicz, M. Famiano, Zhuxia Li, W. G. Lynch, and A. W. Steiner, *Phys. Rev. Lett.* **102**, 122701 (2009).
- [25] J. B. Natowitz, G. Ropke, S. Typel, D. Blaschke, A. Bonasera, K. Hagel, T. Klahn, S. Kowalski, L. Qin, S. Shlomo, R. Wada, and H. H. Wolter, *Phys. Rev. Lett.* **104**, 202501 (2010).
- [26] P. Russotto, P. Z. Wu, M. Zoric, M. Chartier, Y. Leifels, R. C. Lemmon, Q. Li, J. Lukasik, A. Pagano, P. Pawlowski, and W. Trautmann, *Phys. Lett. B* **697**, 471 (2011).
- [27] D. V. Shetty, S. J. Yennello, and G. A. Souliotis, *Phys. Rev. C* **76**, 024606 (2007).
- [28] P. Napolitani, M. Colonna, F. Gulminelli, E. Galichet, S. Piantelli, G. Verde, and E. Vient, *Phys. Rev. C* **81**, 044619 (2010).
- [29] E. Galichet *et al.*, *Phys. Rev. C* **79**, 064614 (2009).
- [30] M. Papa, T. Maruyama, and A. Bonasera, *Phys. Rev. C* **64**, 024612 (2001).
- [31] F. Amorini *et al.*, *Phys. Rev. Lett.* **102**, 112701 (2009).
- [32] A. Pagano *et al.*, *Nucl. Phys. A* **734**, 504 (2004).
- [33] A. Pagano, *Nucl. Phys. News* **22**, 25 (2012).
- [34] N. Le Neindre *et al.*, *Nucl. Instrum. Methods Phys. Res., Sect. A* **490**, 251 (2002).
- [35] M. Alderighi *et al.*, *Nucl. Instrum. Methods Phys. Res., Sect. A* **489**, 257 (2002).
- [36] M. Alderighi *et al.*, *Nucl. Phys. A* **734**, E88 (2004).
- [37] I. Lombardo *et al.*, *Nucl. Phys. A* **834**, 458 (2010).
- [38] I. Lombardo *et al.*, *Int. J. Mod. Phys. E* **19**, 1170 (2010).
- [39] C. Cavata, M. Demoulin, J. Gosset, M.-C. Lemaire, D. L'Hôte, J. Poitou, and O. Valette, *Phys. Rev. C* **42**, 1760 (1990).
- [40] H. Delagrange and J. Peter, *Nucl. Phys. A* **471**, 111 (1987).
- [41] M. Papa and G. Giuliani, *Eur. Phys. J. A* **39**, 117 (2009).
- [42] C. Rizzo, V. Baran, M. Colonna, A. Corsi, and M. Di Toro, *Phys. Rev. C* **83**, 014604 (2011).
- [43] M. Prakash, T. L. Ainsworth, and J. M. Lattimer, *Phys. Rev. Lett.* **61**, 2518 (1988).
- [44] Bao-An Li, Lie-Wen Chen, and Che Ming Ko, *Phys. Rep.* **464**, 113 (2008).
- [45] R. J. Charity, D. R. Bowman and Z. H. Liu, R. J. McDonald, M. A. McMahan, G. J. Wozniak, L. G. Moretto, S. Bradley, W. L. Kehoe, and A. C. Mignerey, *Nucl. Phys. A* **476**, 516 (1988).